Hypoglycemia Detection Based on ear-EEG

Alvaro Fuentes Cabrera (alca@uneeg.com)
UNEEG Medical A/S https://orcid.org/0000-0001-7414-7724
Simon Lind Kappel
Aarhus Universitet
Line Sofie Remvig
UNEEG Medical A/S
Hans Olaf Toft
UNEEG Medical A/S
Rasmus Elsborg Madsen
UNEEG Medical S/A
Preben Kildmose
Aarhus Universitet
Mike Lind Rank
UNEEG Medical A/S

Research

Keywords: Hypoglycemia detection, ear-EEG, wearable EEG, Electroencephalography (EEG)

Posted Date: December 10th, 2020

DOI: https://doi.org/10.21203/rs.3.rs-122971/v1

RESEARCH

Hypoglycemia detection based on ear-EEG

Alvaro Fuentes Cabrera[1*], Simon Lind Kappel[2], Line Sofie Remvig[1], Hans Olaf Toft[1], Rasmus Elsborg Madsen[1], Preben Kidmose[2] and Mike Lind Rank[1]

[*]Correspondence: alca@uneeg.com
[1] UNEEG Medical A/S, Lynge, Denmark
Full list of author information is available at the end of the article

Abstract

Background: Hypoglycemia refers to the condition in which the blood glucose is severely below normal level. Hypoglycemia can cause difficulties to talk, headache, irritability, anxiety, confusion, convulsions, seizures, unconsciousness, and even death. These symptoms are a consequence of insufficient supply of glucose to the brain. It has previously been demonstrated that hypoglycemia results in characteristic changes in the electroencephalographic (EEG) signals recorded from electrodes on the scalp. Scalp EEG is not suitable for continuous measurements, due to its obtrusive nature and limited capabilities for monitoring in real-life environments. The objective of this study was to asses the feasibility of detecting hypoglycemia-induced episodes using EEG signals recorded with dry-contact in-ear electrodes, which are discreet, have the potential for long-term EEG monitoring in real-life situations, and provide similar information to that recorded with scalp EEG.

The data from 5 diabetic subjects were used for this study. Six ear-EEG channels recorded from dry-contact iridium oxide electrodes fitted the right ear, and channels C3, Pz, T7, and T8 were used for the analysis and classification procedures. A Support Vector Machine (SVM) with a linear kernel was used to detect the hypoglycemic episodes, using a normalized measure of the total power of the θ, α, β, and γ frequency bands as features.

Results: The results showed that there were no statistical differences between the sensitivity and specificity of the contralaterally referenced scalp-scalp and ear-scalp EEG channels. Contralaterally referenced channels showed an average sensitivity over all 5 subjects $\geq$90%, SD$\leq$10% and an average specificity over all 5 subjects $\geq$82%, SD$\leq$24%. The sensitivities and specificities obtained with the data from the ipsilaterally referenced ear-ear EEG channels did not exceed chance level.

Trial registration: ClinicalTrials.gov NCT03022058. Registered 13 December 2016 https://clinicaltrials.gov/ct2/show/NCT03022058?term=uneeg&draw=3&rank=12.

Keywords: Hypoglycemia detection; ear-EEG; wearable EEG; Electroencephalography (EEG)

Background

The near-normalisation of glucose levels has become an established goal in diabetes treatment in order to reduce the risk of late complications such as neuropathy, retinopathy and cardiovascular diseases [1]. Hypoglycemia is the most common adverse event associated with insulin treatment in subjects with diabetes [2]. The fear of hypoglycemia discourages subjects from maintaining tight glycemic control. Hence, only a minority of the subjects reach the defined goal of glucose control, leading to increased diabetes related morbidity and mortality [3]–[4].

Electroencephalography (EEG) is an electrophysiological monitoring method to record electrical activity of the brain. This activity reflects the brain's functional state.
The brain is critically dependent on a continuous supply of glucose, and when the glucose level is lower than the metabolic requirements of the brain, brain function deteriorates. Neuroglycopenic hypoglycemia in insulin-treated subjects with diabetes is associated with characteristic changes in EEG, dominated by an increase in theta activity [5]. These changes are clearly seen at blood glucose level of less than ~ 3.4 mmol/L [6, 7] preceding the development of severe cognitive dysfunction [8]. The EEG changes seem to be present irrespective of age, diabetes duration and awareness status towards hypoglycemia [9]. Detection of EEG changes thus constitutes a basis for a biosensor alarm for hypoglycemia detection [10].

Ear-EEG is a method for recording EEG from electrodes placed in and around the ear [11, 12, 13]. The method was mainly developed to enable EEG recording in an unobtrusive and discreet way in the user's everyday life, thereby enabling real life brain monitoring [14]. The feasibility of the method has been established through well-known event-related potentials such as auditory evoked potentials [15], P300 [16], auditory steady-state responses (ASSR) [17, 18] and mismatch negativity [18]. Ear-EEG has been applied to a variety of medical applications including hearing threshold estimation [19, 17], epileptic seizures detection [20], sleep staging [21, 22] and brain-computer interfaces [23, 24, 25].

The main advantage of ear-EEG is the potential for developing discreet and user-friendly devices enabling real life brain monitoring. However, the majority of previously published results were recorded with wet electrodes requiring application of electrode gel or similar electrolytes. To advance the user-friendliness and comfort

of ear-EEG devices, it has recently been demonstrated that ear-EEG signals can be recorded using dry-contact electrodes embedded on a customized earpiece [26].

A potential medical application of an ear-EEG system is the detection of hypoglycemia-induced changes in the EEG in subjects with Type 1 diabetes. To our knowledge, no studies have investigated the detection of hypoglycemic episodes by use of ear electrodes. While a finger prick test accurately measures the blood glucose level, it does not provide continuous measurements, thus the user must be proactive, and hence it is unreliable as a hypoglycemia alarm. Recent studies have indicated that the use of continuous glucose monitoring (CGM) reduces the risk of severe hypoglycemia [27, 28]. However, some find these devices troublesome to use. Observational data show that only a small percentage of subjects with Type 1 diabetes are using CGM on an ongoing basis [29]. Thus, there is a medical need for a reliable hypoglycemia detection device which is easy and convenient to use.
This clinical study aimed at investigating the feasibility of detecting hypoglycemia-induced episodes using ear-EEG, and to compare these results with those achieved using EEG recorded from scalp electrodes.

Materials and Methods

Subjects

Five subjects between 37-70 years old (1 woman and 4 men), diagnosed with Type 1 diabetes for $\geq$ 5 years, were included in this study[1]. All subjects gave their written consent to participate in the experiment. Exclusion criteria were severe cardiac disease, uremia, liver disease, epilepsy, known or suspected abuse of alcohol, or neuroactive substances, cochlear implants, narrow or malformed ear canal, pregnancy, subjects that were incapable of understanding the subject information, or subjects using any of the following drugs: Chemotherapeutic drugs of any kind, methotrexate, third generation anti-psychotic drugs (aripiprazole, quetiapine, clozapine, ziprasidone, paliperidone, risperidone, sertindole, amisulpride, olanzapine).

Ear-EEG Device

Ear-EEG were recorded from customized silicone earpieces with 6 iridium oxide (IrO_2) dry electrodes embedded on the surface [26, 12]. The earpieces were manufactured using bio-compatible materials.

[1]Nine subjects participated in this experiment, but the EEG data from four of them contained a large number of artifacts due to cable movement, and/or no data due to poor electrode contact, and therefore they were not included in subsequent data analysis.

EEG Recordings

All scalp EEG and ear-EEG were recorded concurrently using a Mobita amplifier (TMSi, The Netherlands), with a sampling frequency $f_s = 2000$ Hz. The same type of IrO_2 electrodes were used in the earpiece and on the scalp. To assist the positioning of the scalp electrodes, the electrodes were embedded into a cap (ECI Electro Cap), modified with two holes for the ears to pass through.

Twenty-four scalp electrodes and six ear electrodes were recorded using the Mobita amplifier. Scalp electrodes were placed according to the international 10/20 system (Fp1, Fpz, Fp2, F7, F3, Fz, F4, F8, FT9, FT10, T7, C3, Cz, C4, T8, P7, P3, Pz, P4, P8, O1, O2, M1, M2), and conductive electrode gel (ECI Electro Gel) was applied from the outside of the cap. Six dry-contact electrodes were mounted in both a left and a right custom-made soft earpiece according to the scheme proposed in [12]. The electrodes covered both the ear canal and the concha region of the ear. The right ear electrodes, labelled ERA, ERB, ERC, ERF, ERK and ERT, were connected to the same am plifier as the scalp electrodes. The left ear was reserved for validation of a proprietary amplifier, which did not have galvanic connection to the Mobita amplifier; the recordings from the left ear electrodes were not used in the analysis presented in this paper.

Glucose Control Paradigm

All five subjects had normal meals previous to the experiment. Intravenous catheters were inserted in both antecubital veins for injection of insulin, infusion of glucose and blood glucose measurements. Glucose solution 200 g/L was readily available in case the subject needed instant glucose infusion. In order to assure collection of good quality EEG "baseline" data, EEG were recorded in the normoglycemic state (5–6 mmol/L) for $\geq$ 1 h before inducing hypoglycemia. For the insulin infusion procedure, 10 ml of the subject's blood was mixed with 500 ml isotonic NaCl (9 g/l) for 10 min. Subsequently, 50 IU Actrapid (100 IU/ml, Novo Nordisk) was added and the solution was mixed for 30 min. If needed, glucose was given orally to keep the range. However, the normoglycemic range was expanded for some subjects. Following at least 1 h of normoglycemia a gradual decrease in glucose infusion was to be performed to obtain a steady decrease in plasma glucose of 3 mmol/L/h. Glucose infusion was only given when the experiment was terminated.
Blood glucose was measured at least every 10 min until it reached 5 mmol/L, and thereafter at least every 5 min. The experiment was terminated when:

1 Blood glucose <1.8 mmol/L by two consecutive measurements

2 The subject was severely affected by hypoglycemia (signs of neuroglycopenia such as speech velocity, alertness, unable to count backward or signs of adrenergic reactions, i.e. shivering and sweating)
3 The subject wanted to discontinue the procedure
4 If the investigator found that continuation of insulin infusion and further lowering of blood glucose would compromise the safety of the subject

The subject continued to stay at the research unit for 1 hour after the hypoglycemia procedure had been stopped, the blood glucose had been >5 mmol/L for at least 30 minutes and the subject was cognitively intact.

Hypoglycemia labeling

The EEG segments recorded during the normoglycemic state were labeled according to the blood glucose measurements (blood glucose >5 mmol/L) and the hypoglycemia episodes were labeled by an expert from UNEEG medical, based on visual inspection of the C3-Pz time-frequency plots. The expert did not have access to the ear-EEG data, and did not participate in neither the signal processing nor the classification process. Normoglycemic segments were label as "non-hypo", hypoglycemic segments were labeled as "hypo", while all remaining segments were labeled as "unlabeled" as shown in the bottom plots of Figures 1 and 2. Table 1 shows the number of normoglycemic, hypoglycemic, unlabeled, and rejected segments for channel ERK-T7 and all 5 subjects.

Data Sets

Each data set was a subset of 32 EEG channels (6 right ear ear-EEG and 24 scalp EEG). These EEG time series correspond to a normoglycemic segment followed by a hypoglycemia segment. Three different data sub-sets were used in this analysis:

1 Four bipolar ear-scalp EEG channels, namely ERF-T7, ERK-T7, ERF-T8, and ERK-T8. The results obtained with the data collected from ERK-T7 and ERF-T7 will serve as an indicator of how crossed ear-EEG channels would perform.
2 Two bipolar scalp-scalp EEG channels, namely C3-Pz and T7-T8. The results obtained with the data collected from these channels will be used as reference for the ear-scalp bipolar channels.
3 Right ear-EEG bipolar channels ERK-ERT, ERF-ERT, ERA-ERT, ERK-ERF, ERK-ERA, ERK-ERB, ERF-ERA, and ERF-ERB. There were 15 possible bipolar combinations, but only 8 of them were available for 4 of the 5 subjects.

EEG data from each of these channels were segmented into 30 s segments with 15 s overlap between segments, for both individual and general classification (see section Classification).

Signal Processing

Figure 3 shows a flow diagram of the signal processing applied[2] to the EEG signals. The raw EEG signals were band-pass filtered between 0.5 Hz and 45 Hz, using a IIR Butterworth filter of order 20 and an approximate roll-off slope of 60 dB/octave. Subsequently, the filtered signals were downsampled to 250Hz, and segmented into 30 s segments with 15 s overlap between segments. In the artifact rejection module, segments with zero amplitude in all 4 frequency bands were rejected and labeled as "unlabeled". These segments correspond to periods when the amplifier was disconnected due to either technical or practical issues related to the EEG system or the subject. For the segments that contained EEG data, all samples $|x_a| > 100\mu V$ were labeled as artifacts. Preceding and subsequent segments were also labeled as artifacts until a segment containing a zero-crossing was located. Segments containing more than 20 % artifacts were discarded, and labeled as "unlabeled". All "unlabeled" segments were not included in the training set of the classifier. For the test procedure, the classifier results for these segments were plotted as red crosses, as can be seen in the bottom plots of Figure 1 and 2. The selected EEG traces (previously re-referenced as described in section Data Sets) were band-pass filtered using IIR Butterworth filters of order 10. Four frequency bands were extracted corresponding to Theta (4-8Hz), Alpha (8-12Hz), Beta (12-30Hz), and Gamma (30-45Hz). The root mean square (RMS) of each frequency band, $E_b(\Delta f)$, was calculated according to Eq. 1, and used as features to feed the classifier described in section Classification.

$$E_b(\Delta f) = \sqrt{\frac{1}{N}\sum_{n=1}^{N} b_{\Delta f}^2[n]} \tag{1}$$

where N is the segment length in samples, $b_{\Delta f}$ are the band-pass filtered time series, with $\Delta f = \theta, \alpha, \beta$, and γ.

Classification

The classifier was a support vector machine (SVM) with a linear kernel[3], and it was fed with the features E_b, described in section Signal Processing. Each data

[2] All processing done using Matlab R2017a
[3] Support Vector Machine toolbox for Matlab Version 2.51, by Anton Schwaighofer.

set described in section Data Sets was used to train an across-subjects classifier, trained with a balanced data set (same number of segments for normoglycemic and hypoglycemic states) from 4 of the 5 subjects, and it was tested with the data corresponding to the one subject not included in the training set (repeated until all subjects were used as test set). The entire data set contained more normoglycemic than hypoglycemic segments (see Table 1), since the recording time for the hypoglycemic state was shorter than for the normoglycemic state. In order to get a balanced data set for training, the normoglycemic segment of the training set was pseudo-randomly selected from the entire normoglycemic period, with a length matching that of the hypoglycemic segment. This procedure was repeated 10 times, to generate 10 training and classification procedures, with different training data for each procedure. The final classification accuracy for this classifier was calculated as the average of all 10 iterations. The test set for the across-subject classifier always contained all available data, thus the normoglycemic segment was always larger than the hypoglycemic segment.

Sensitivity and specificity were calculated for the results obtained with the SVM. The sensitivity index represents the accuracy with which the SVM detects the hypoglycemic segments, while the specificity index will give the reader an estimate of how well the SVM detects the normoglycemic segments. These two indexes are defined in equations 2 and 3.

$$Sensitivity = \frac{TP}{TP + FN} \cdot 100 \tag{2}$$

$$Specificity = \frac{TN}{TN + FP} \cdot 100 \tag{3}$$

where TP (true positive) denotes the number of correctly detected hypoglycemic segments, FN (false negative) is the number of wrongly detected normoglycemic segments, TN (true negative) is the number of correctly detected normoglycemic segments, and FP (false positive) is the number of wrongly detected hypoglycemic segments.

Sensitivy and specificity results from all ERF and ERK channels referenced to T7 and T8 were tested against C3-Pz and T7-T8 using a t-test with significance level 5%.

Results

Figure 1 shows the data and the classification results for subjects 1, 2, 3 and 4 from one bipolar EEG channel (ERK-T7). Each subject is represented by three panels: The top panel shows the RMS value for each of the four frequency bands as a function of time. Each color block represents the RMS value of a 30 s segment, with an overlap of 15 s. Due to large differences in amplitude of the different frequency bands, the RMS values were normalized to the highest RMS value within each band. This procedure was only performed for a better visualization of the amplitude changes in time and it was not part of the signal processing and classification system. The middle panel shows the measured plasma glucose values. The bottom panel shows the expert labels for each of the 30s segments (blue line), the rejected segments (red crosses), and the output of the classifier (green crosses).

Figure 2 shows the data and classification results for subject 5 using the same three panels as described for Figure 1. Subject 5 will be described and analyzed separately due to the large number of segments rejected by the rejection algorithm.

The classifiers was trained based on a leave-one-subject-out scheme. Thus, the classifier for subject 1 was trained on data from subject 2, 3, 4 and 5, the classifier for subject 2 was trained on data from subject 1, 3, 4 and 5, and so on.

Figure 1 and 2 show the data and classification from channel ERK-T7 ; the same analysis was performed for 5 other bipolar channels (C3-Pz, T7-T8, ERF-T7, ERK-T8, and ERF-T8).

Figure 4 summarizes the classification results for all 5 subjects for the 6 selected bipolar EEG channels. The plot shows both the individual classification performance as well as the statistics over the 5 subjects represented as the average, standard deviation and 95% confidence interval. The top panel shows the specificity, whereas the bottom panel shows the sensitivity.

Discussions

Since the classification results for the ipsilaterally referenced ear-ear EEG channels did not give results above chance, only the sensitivity and specificity for the scalp-scalp and ear-scalp EEG channel will be discussed in this section.

The SVM classifier is able to detect the hypoglycemic episodes for all 5 subjects, for the scalp-scalp and ear-scalp EEG channels, as seen in Figure 4, where it can also be observed that the sensitivity results obtained with the data collected from ERK-T7, ERF-T7, and T7-T8 (average sensitivity over all 5 subjects $\geq$90%, SD$\leq$10%) show considerably less variability than those obtained with C3-Pz, ERF-T8, and ERK-T8 (average sensitivity over all 5 subjects between 67- 82%, SD$\geq$26%). The specificity

results obtained with the data collected from C3-Pz, T7-T8, ERK-T7, and ERF-T8 show average specificities over all 5 subjects $\geq$82%, SD$\leq$24%, while ERK-T8 and ERF-T8 show average specificities over all 5 subjects $\leq$76%, SD$\geq$37%. According to these results, the ear electrodes referenced to T8 (ipsilateral temporal lobe), show greater variability and lower sensitivity/specificity than the ear electrodes referenced to T7 (contralateral temporal lobe) and the two scalp-scalp channels (C3-Pz and T7-T8). Previous studies suggest a difference in sensitivity to hypoglycemia between the anterior and posterior cortices [30, 31], but no major interhemispheric asymmetry has been reported [30, 32] that could explain the difference in classification performance between ERX-T7 and ERX-T8.

Figure 2 shows the features, blood plasma, and SVM output for Subject 5, channel ERK-T7. It can be seen in the bottom plot, that a large number of segments were rejected due to artifacts, which is reflected on the high amplitudes in all 4 frequency bands displayed in the top plot. Very similar features and number of rejected segments were found for channels ERF-T7, ERK-T8, and ERF-T8. While the specificity for channel ERK-T7 is approximately 40% (the lowest for this channel), other channels with a large number of rejected segments reached specificity percentages of 87% (ERF-T7) and 76 % (ERF-T8), suggesting that there is no direct relation between EEG artifacts and specificity.

The plasma glucose threshold for hypoglycemia detection changes across subjects from 2-4 [mmol/l], as observed in Figures 1 and 2. For example, while a clear hypoglycemia detection is achieved around minute 180 for Subject 1 (approximately 4 [mmol/l]), for Subject 2 the detection is not clear until after minute 220 (approximately 2.2 [mmol/l]). These results suggest an individual critical glucose threshold for the onset of EEG changes, as also reported by [5].

The results obtained with the ear channels referenced to T7 are a good indicator of of how a classifier would perform using data collected from a bipolar EEG channel derived between the two ears.

No significant differences were observed between the specificity and sensitivity results for the ear-scalp EEG channels and the scalp-scalp EEG channels, according to a t-test with significance level 5%.

Acknowledgments

We would like to thank Ewa Romanczuk, Lone Hansen, Eva-Marie Margareta Gram-Kampmann, and Vibe Vestergaard from Odense University Hospital for assisting with the insulin delivery to the subjects subjects participating in the study, Thomas Ølund from UNEEG Medical for labeling the hypoglycemic events, and the clinical affairs department of UNEEG Medical for reviewing this manuscript.

Funding

This research was supported by Innovation Fund Denmark (j.nr. 110-2013-1)

Abbreviations

EEG: Electroencephalohraphy, **SVM**: Support vector machine, **ASSR**: Auditory steady-state responses, **CGM**: Continuous glucose monitoring, **SVM**

Availability of data and materials

Data are available from the author upon reasonable request.

Ethics approval and consent to participate

The study was designed and conducted in accordance with the International Standards Organization 14155 and the principles of the Declaration of Helsinki (1964, and its amendments and subsequent clarifications) [33], and approved by the Regional Committees on Health Research Ethics for Southern Denmark and the Danish Medicines Agency with project-ID S-20160192.

Competing interests

The authors declare that they have no competing interests.

Consent for publication

Not applicable.

Competing interests

The authors declare that they have no competing interests.

Authors' contributions

AFC, PK, and MLR wrote the manuscript and designed the algorithm. AFC wrote the code for feature extraction and classification. LSR, SLK, PK, HOT, MLR, and REM designed the experiment setup and protocol, and reviewed the manuscript. HOT, MLR, SLK, PK: designed the hardware setup and measurement system.

Author details

[1] UNEEG Medical A/S, Lynge, Denmark. [2] Department of Engineering, Aarhus University, Aarhus, Denmark.

References

1. Control, D., Group, C.T.R., Nathan, D., Genuth, S., Lachin, J., Cleary, P., Crofford, O., Davis, M., Rand, L., Siebert, C.: The effect of intensive treatment of diabetes on the development and progression of long-term complications in insulin-dependent diabetes mellitus. New England Journal of Medicine **329**(14), 977–986 (1993). doi:10.1056/NEJM199309303291401
2. Wild, D., von Maltzahn, R., Brohan, E., Christensen, T., Clauson, P., Gonder-Frederick, L.: A critical review of the literature on fear of hypoglycemia in diabetes: Implications for diabetes management and patient education. Patient Education and Counseling **68**(1), 10–15 (2007). doi:10.1016/j.pec.2007.05.003
3. Control, T.D., Group, C.T.R.: Hypoglycemia in the diabetes control and complications trial. Diabetes **46**(2), 271–286 (1997). doi:10.2337/diab.46.2.271. http://diabetes.diabetesjournals.org/content/46/2/271.full.pdf
4. Karges, B., Rosenbauer, J., Kapellen, T., Wagner, V.M., Schober, E., Karges, W., Holl, R.W.: Hemoglobin a1c levels and risk of severe hypoglycemia in children and young adults with type 1 diabetes from germany and austria: A trend analysis in a cohort of 37,539 patients between 1995 and 2012. PLOS Medicine **11**(10), 1–9 (2014). doi:10.1371/journal.pmed.1001742
5. Blaabjerg, J., Juhl, C.: Hypoglycemia-induced changes in the electroencephalogram: An overview. J Diabetes Sci Technol. **10**(6), 1259–1267 (2016). doi:10.1371/journal.pmed.1001742
6. Pramming, S., Thorsteinsson, B., Stigsby, B., Binder, C.: Glycaemic threshold for changes in electroencephalograms during hypoglycaemia in patients with insulin dependent diabetes. Br Med J (Clin Res Ed). **296**(6623), 665–667 (1988)
7. Tallroth, G., Lindgren, M., Stenberg, G., Rosen, I., Agardh, C.: Neurophysiological changes during insulin-induced hypoglycaemia and in the recovery period following glucose infusion in type 1 (insulin-dependent) diabetes mellitus and in normal man. Diabetologia **33**(5), 319–323 (1990)
8. Howorka, K., Heger, G., Schabmann, A., Anderer, P., Tribl, G., Zeitlhofer, J.: Severe hypoglycaemia unawareness is associated with an early decrease in vigilance during hypoglycaemia. Psychoneuroendocrinology **21**(3), 295–312 (1996)
9. Remvig, L., Elsborg, R., Sejling, A., Sørensen, J., Snogdal, L.S., Folkestad, L., Juhl, C.: Hypoglycemia-related electroencephalogram changes are independent of gender, age, duration of diabetes, and awareness status in type 1 diabetes. J Diabetes Sci Technol. **6**(6), 1337–44 (2012)
10. Elsborg, R., Remvig, L., H, H.B.-N., Juhl, C.: Detecting hypoglycemia by using the brain as a biosensor. In: Serra, P.A. (ed.) Biosensors for Health, Environment and Biosecurity, pp. 201–213. IntechOpen, ??? (2011).

https://www.intechopen.com/books/biosensors-for-health-environment-and-biosecurity/detecting-hypoglycemia-by-using-the-brain-as-a-biosensor

11. Looney, D., Kidmose, P., Park, C., Ungstrup, M., Rank, M., Rosenkranz, K., Mandic, D.: The in-the-ear recording concept. IEEE Pulse **3**(6), 32–42 (2012)
12. Kidmose, P., Looney, D., Ungstrup, M., Rank, M., Mandic, D.: A study of evoked potentials from ear-EEG. IEEE Transactions on Bio-Medical Engineering **60**(10), 2824–30 (2013)
13. Debener, S., Emkes, R., Vos, M.D., Bleichner, M.: Unobtrusive ambulatory EEG using a smartphone and flexible printed electrodes around the ear. Scientific reports 5 (2015)
14. Kappel, S.L.: Development and Characterization of Ear-EEG for Real-Life Brain-Monitoring. PhD thesis, department of engineering, Aarhus University (September 2016). doi:10.7146/aul.260.183
15. Kidmose, P., Looney, D., Mandic, D.: Auditory evoked responses from ear-EEG recordings. Conf Proc IEEE Eng Med Biol Soc., 586–589 (2012). doi:10.1109/EMBC.2012.6345999
16. Kaongoen, N., Jo, S.: An auditory p300-based brain-computer interface using ear-EEG. 2018 6th International Conference on Brain-Computer Interface (BCI) (2018). doi:10.1109/IWW-BCI.2018.8311519
17. Christensen, C., Harte, J., Lunner, T., Kidmose, P.: Ear-EEG based objective hearing threshold estimation evaluated on normal hearing subjects. IEEE Transactions on Biomedical Engineering **65**(5), 1026–1034 (2018)
18. Mikkelsen, K., Kappel, L., Mandic, D., Kidmose, P.: EEG recorded from the ear: Characterizing the ear-EEG method. Front. Neurosci. **9**(438), 1337–44 (2015). doi:0.3389/fnins.2015.00438
19. Christensen, C., Hietkamp, R., Harte, J., Lunner, T., Kidmose, P.: Toward EEG-assisted hearing aids: Objective threshold estimation based on ear-EEG in subjects with sensorineural hearing loss. Trends Hear (2018)
20. Zibrandtsen, I., Kidmose, P., Christensen, C., Kjaer, T.: Ear-EEG detects ictal and interictal abnormalities in focal and generalized epilepsy - a comparison with scalp EEG monitoring. Clin Neurophysiol. **128**(12), 2454–2461 (2017)
21. Mikkelsen, K., Villadsen, D., Otto, M., Kidmose, P.: Automatic sleep staging using ear-EEG. Biomed Eng Online. **16**(111) (2017). doi:10.1186/s12938-017-0400-5
22. Mikkelsen, K., Tabar, Y., Kappel, S., Christensen, C., Toft, H., Hemmsen, M., Rank, M., Otto, M., Kidmose, P.: Accurate whole-night sleep monitoring with dry-contact ear-EEG. Sci Rep **9**(16824) (2019). doi:10.1038/s41598-019-53115-3
23. Ahn, J., Ku, Y., Kim, D., Sohn, J., Kim, J., Kim, H.: Wearable in-the-ear EEG system for ssvep-based brain–computer interface. Electronics Letters **54**(7), 413–414 (2018)
24. Wang, Y., Nakanishi, M., Kappel, S., Kidmose, P., Mandic, D., Wang, Y., Cheng, C., Jung, T.: Developing an online steady-state visual evoked potential-based brain-computer interface system using ear-EEG. Conf Proc IEEE Eng Med Biol Soc, 2271–2274 (2015). doi:10.1109/EMBC.2015.7318845
25. Farooq, F., Looney, D., Mandic, D., Kidmose, P.: Ear-EEG based visual p300 brain-computer interface. 2015 7th International IEEE/EMBS Conference on Neural Engineering (NER) (2015). doi:10.1109/NER.2015.7146569
26. Kappel, L., Rank, M., Toft, H., Andersen, M., Kidmose, P.: Dry-contact electrode ear-EEG. IEEE Trans. Biomedical Engineering **66**(1), 150–158 (2018). doi:10.1109/TBME.2018.2835778
27. Choudhary, P., Ramasamy, S., Green, L., Gallen, G., Pender, S., Brackenridge, A., Amiel, S.A., Pickup, J.C.: Real-time continuous glucose monitoring significantly reduces severe hypoglycemia in hypoglycemia-unaware patients with type 1 diabetes. Diabates Care **12**(438), 4160–62 (2013)
28. Tamborlane, W., Beck, R., Bode, B., Buckingham, B., Chase, H., Clemons, R., Fiallo-Scharer, R., Fox, L., Gilliam, L., Hirsch, I., Huang, E., Kollman, C., Kowalski, A., Laffel, L., Lawrence, J., Lee, J., Mauras, N., O'Grady, M., Ruedy, K., Tansey, M., Tsalikian, E., Weinzimer, S., Wilson, D., Wolpert, H., Wysocki, T., Xing, D.: Continuous glucose monitoring and intensive treatment of type 1 diabetes. N Engl J Med. **359**(14), 1464–76 (2008). doi:10.1056/NEJMoa0805017
29. Rodbard, D.: A review of successes, challenges, and opportunities. Diabetes Technol Ther. **18**(suppl 2), 3–13 (2016). doi:10.1089/dia.2015.0417
30. Bjørgaas, M., Sand, T., Vik, T., Jorde, R.: Quantitative EEG during controlled hypoglycaemia in diabetic and non-diabetic children. Diabet Med. (15), 30–37 (1998)
31. Tamburrano, G., Lala, A., Locuratolo, N., Leonetti, F., Sbraccia, P., Giaccari, A., Busco, S., Porcu, S.: Electroencephalography and visually evoked potentials during moderate hypoglycemia. J Clin Endocrinol Metab. (66), 1301–1306 (1988)
32. Tribl, G., Heger, K.H.G., Anderer, P., Thoma, H., Zeitlhofer, L.: EEG topography during insulin-induced hypoglycemia in patients with insulin-dependent diabetes mellitus. Eur Neurol. (36), 303–309 (1996)
33. Association, W.M.: World medical association declaration of helsinki: Ethical principles for medical research

involving human subjects. JAMA **310**(20), 2191–4 (2013). doi:10.1109/TBME.2018.2835778

Figures

Figure 1 Examples of the normalized features from a bipolar EEG channel (ERK-T7) for subjects 1,2,3, and 4, and their respective classifier outputs. For each subfigure (A,B,C, and D) the subplots are divided as Top: Features from the test set, (these data was not included in the training phase of the SVM), calculated as described in section Signal Processing. Middle: subject's plasma glucose measured as described in section Glucose Control Paradigm. Bottom: The blue line represents the normoglycemic state and hypoglycemia segments as labeled by the UNEEG Medical's expert. The green crosses represent the output of the SVM, for the features in the top plot, and the red crosses represent the segments rejected due to artifacts.

Figure 2 Example of the normalized features from a bipolar EEG channel (ERK-T7, subject 5) with a large number of rejected segments due to noise. Top: Features from the test set, (these data was not included in the training phase of the SVM), calculated as described in section Signal Processing. The blue segments correspond to periods during which the amplifier was turned off to replace the battery. Middle: subject's plasma glucose measured as described in section Glucose Control Paradigm. Bottom: The blue line represents the normoglycemic state and hypoglycemia segments as labeled by the UNEEG Medical's expert. The green crosses represent the output of the SVM, for the features in the top plot, and the red crosses represent the segments rejected due to artifacts.

Figure 3 Flow diagram of the algorithm applied to data from bipolar EEG channels.

Figure 4 Classification results, displayed as individual percentages (color dots), mean $\pm$ standard deviation (error bars), and upper and lower 95% confidence interval (red triangles). Top: Specificity. Bottom: Sensitivity.

Tables

Table 1 Number of normoglycemic and hypoglycemic segments for channel ERK-T7 and all 5 subjects.

	Subject				
Label	1	2	3	4	5
Hypoglycemic	123	37	245	137	154
Normoglycemic	317	508	284	366	385

Figures

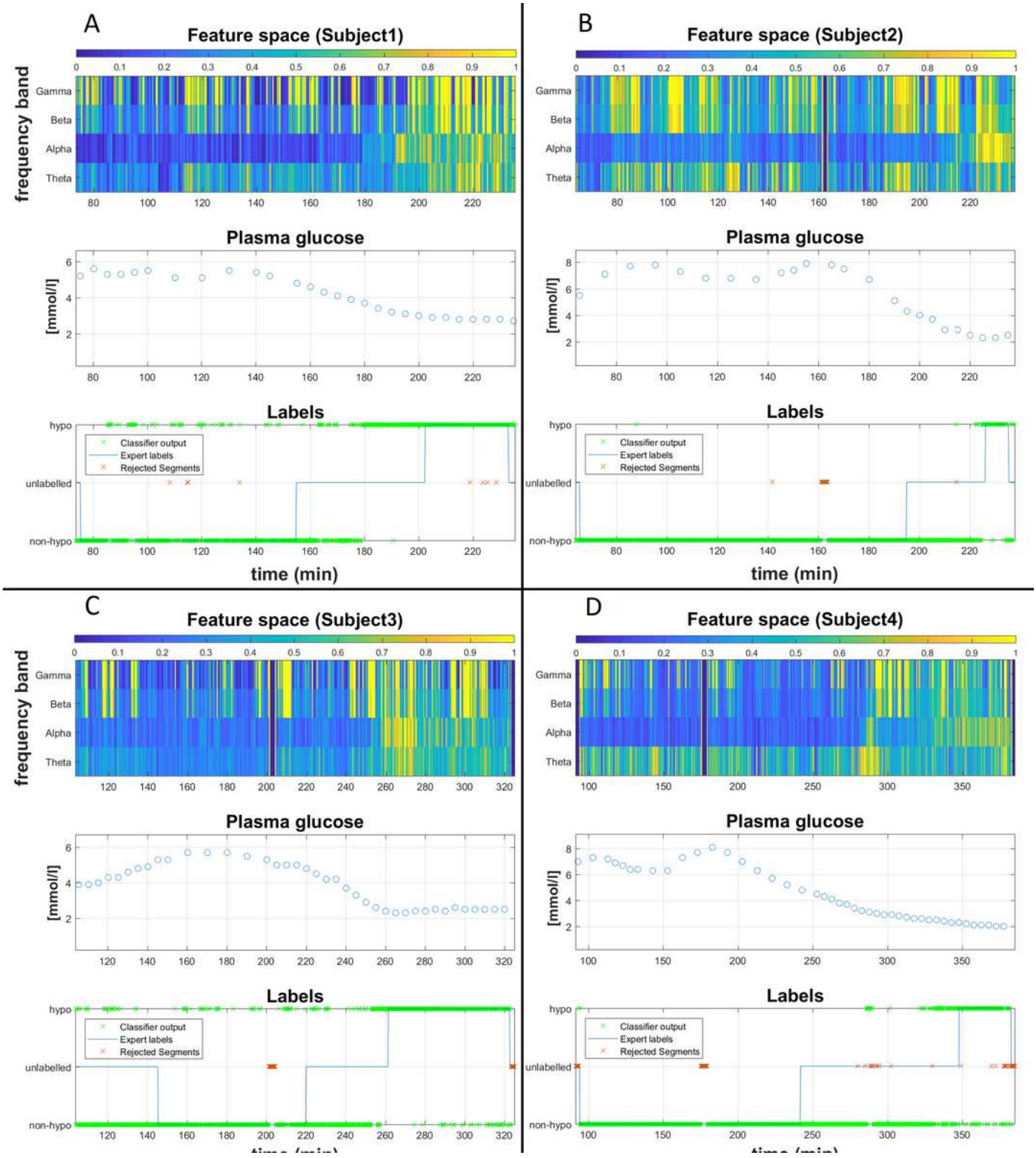

Figure 1

Examples of the normalized features from a bipolar EEG channel (ERK-T7) for subjects 1,2,3, and 4, and their respective classifier outputs. For each subfigure (A,B,C, and D) the subplots are divided as Top: Features from the test set, (these data was not included in the training phase of the SVM), calculated as

described in section Signal Processing. Middle: subject's plasma glucose measured as described in section Glucose Control Paradigm. Bottom: The blue line represents the normoglycemic state and hypoglycemia segments as labeled by the UNEEG Medical's expert. The green crosses represent the output of the SVM, for the features in the top plot, and the red crosses represent the segments rejected due to artifacts.

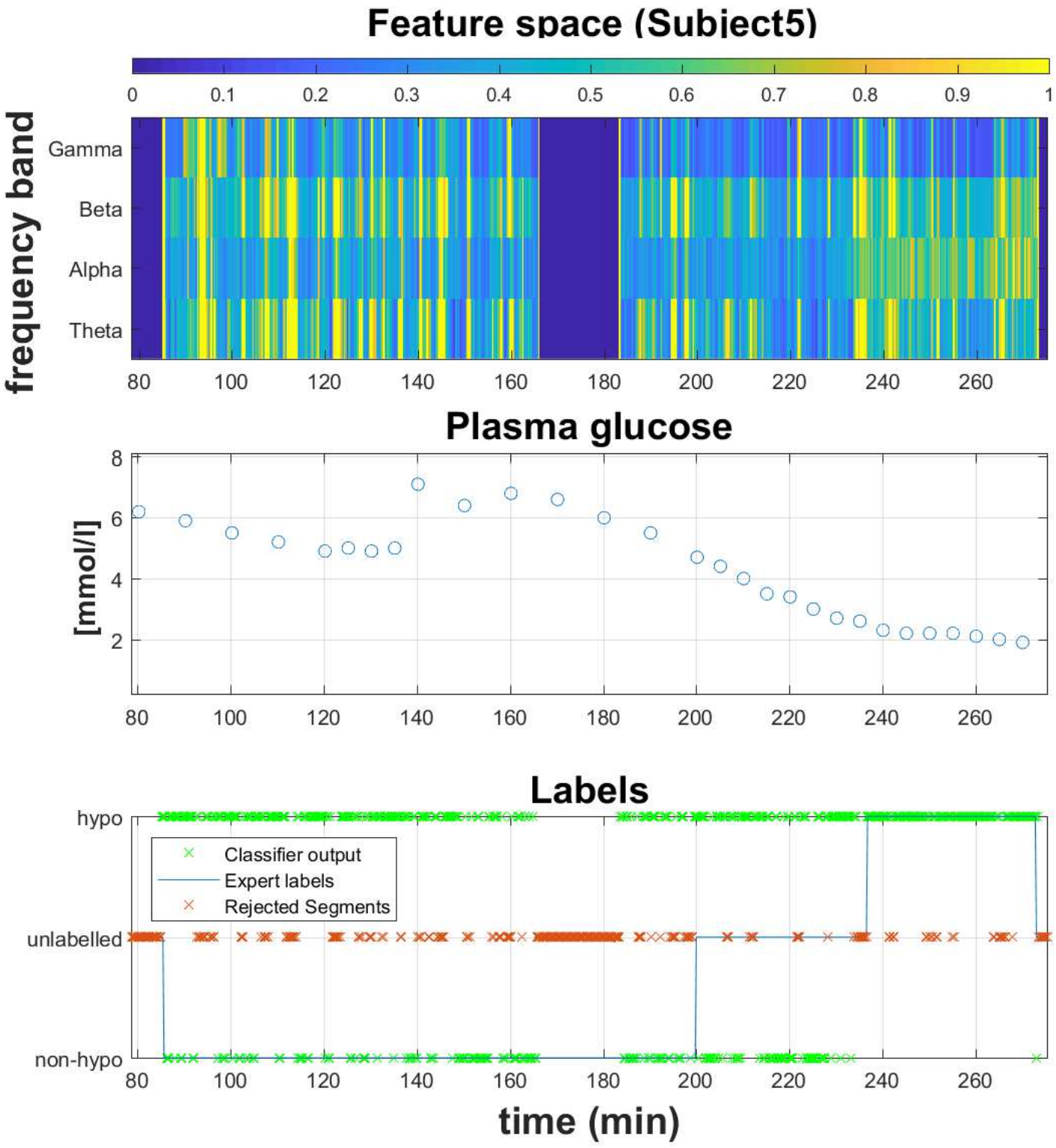

Figure 2

Example of the normalized features from a bipolar EEG channel (ERK-T7, subject 5) with a large number of rejected segments due to noise. Top: Features from the test set, (these data was not included in the training phase of the SVM), calculated as described in section Signal Processing. The blue segments correspond to periods during which the amplifier was turned off to replace the battery. Middle: subject's plasma glucose measured as described in section Glucose Control Paradigm. Bottom: The blue line represents the normoglycemic state and hypoglycemia segments as labeled by the UNEEG Medical's expert. The green crosses represent the output of the SVM, for the features in the top plot, and the red crosses represent the segments rejected due to artifacts.

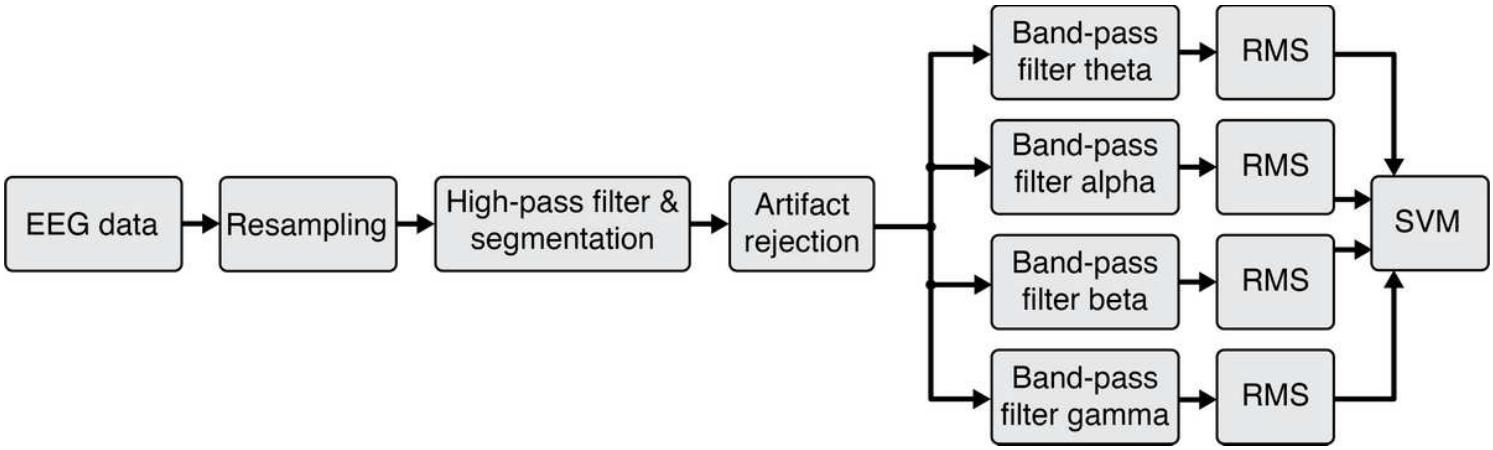

Figure 3

Flow diagram of the algorithm applied to data from bipolar EEG channels.

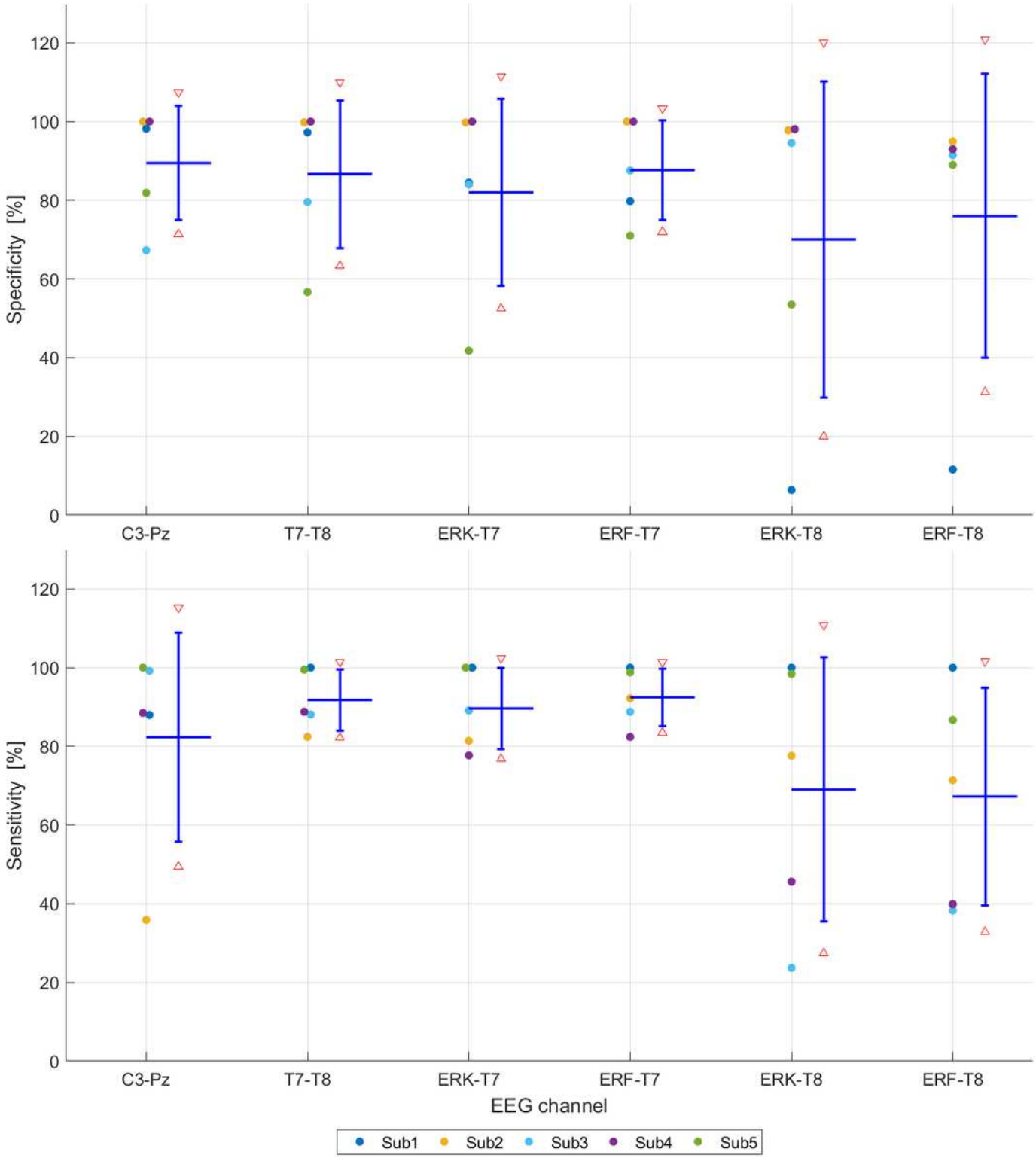

Figure 4

Classification results, displayed as individual percentages (color dots), mean ± standard deviation (error bars), and upper and lower 95% confidence interval (red triangles). Top: Specificity. Bottom: Sensitivity.